

Nitric Oxide Increases Cardiac I_{K1} by Nitrosylation of Cysteine 76 of Kir2.1 Channels

Ricardo Gómez,* Ricardo Caballero,* Adriana Barana, Irene Amorós, Enrique Calvo, Juan Antonio López, Helene Klein, Miguel Vaquero, Lourdes Osuna, Felipe Atienza, Jesús Almendral, Ángel Pinto, Juan Tamargo, Eva Delpón

Rationale: The cardiac inwardly rectifying K^+ current (I_{K1}) plays a critical role in modulating excitability by setting the resting membrane potential and shaping phase 3 of the cardiac action potential.

Objective: This study aims to analyze the effects of nitric oxide (NO) on human atrial I_{K1} and on Kir2.1 channels, the major isoform of inwardly rectifying channels present in the human heart.

Methods and Results: Currents were recorded in enzymatically isolated myocytes and in transiently transfected CHO cells, respectively. NO at myocardial physiological concentrations (25 to 500 nmol/L) increased inward and outward I_{K1} and $I_{Kir2.1}$. These effects were accompanied by hyperpolarization of the resting membrane potential and a shortening of the duration of phase 3 of the human atrial action potential. The $I_{Kir2.1}$ increase was attributable to an increase in the open probability of the channel. Site-directed mutagenesis analysis demonstrated that NO effects were mediated by the selective S-nitrosylation of Kir2.1 Cys76 residue. Single ion monitoring experiments performed by liquid chromatography/tandem mass spectrometry suggested that the primary sequence that surrounds Cys76 determines its selective S-nitrosylation. Chronic atrial fibrillation, which produces a decrease in NO bioavailability, decreased the S-nitrosylation of Kir2.1 channels in human atrial samples as demonstrated by a biotin-switch assay, followed by Western blot.

Conclusions: The results demonstrated that, under physiological conditions, NO regulates human cardiac I_{K1} through a redox-related process. (*Circ Res.* 2009;105:383-392.)

Key Words: nitric oxide ■ Kir2.1 channels ■ resting membrane potential ■ cardiac myocytes ■ I_{K1}

The hallmark of the cardiac inwardly rectifying K^+ current (I_{K1}) is the strong inward rectification; that is, the preferential conduction of inward compared to outward current.¹ I_{K1} provides a large inward conductance at membrane potentials below the reversal potential of K^+ (E_K), and a relatively large outward conductance at potentials just above E_K , which helps to maintain the resting membrane potential (RMP) close to E_K and controls the approach to threshold on depolarization. In contrast, I_{K1} channels remain closed throughout the plateau phase of the cardiac action potential (AP), which permits relatively small inward currents to maintain the plateau. Thereafter, on repolarization (at potentials negative to -20 mV), I_{K1} provides substantial K^+ efflux to contribute to phase 3 of repolarization.² Therefore, I_{K1} plays a critical role in modulating cardiac excitability by setting the diastolic RMP and shaping the initial depolarization and the final repolarization phases of the AP in both atria and ventricles.²

In the human heart, 3 inwardly rectifying channels (Kir2.1, Kir2.2, and Kir2.3) contribute to I_{K1} .³ Experimental data suggest that the Kir2.1 channel is the major isoform underlying ventricular I_{K1} , whereas its relative contribution to atrial I_{K1} seems to be lower.⁴ In fact, gain- and loss-of-function mutations in the gene encoding Kir2.1 (KCNJ2) have been reported to cause short QT and long QT (Andersen-Tawil) syndromes, respectively.⁵ Both syndromes, particularly the former, are associated with severe ventricular arrhythmias. Indeed, the importance of I_{K1} in the establishment of a fast and stable reentry of spiral waves (rotors) and ventricular fibrillation dynamics has been demonstrated.⁶

Nitric oxide (NO) is a gaseous mediator produced by all myocardial cell types. In the heart, NO plays an important role in regulating rate, contractile function, coronary tone, myocardial oxygen consumption, mitochondrial respiration, autonomic signaling, and cell growth and survival.⁷ Using conventional microelectrode techniques, we recently de-

Original received November 7, 2008; resubmission received March 19, 2009; revised resubmission received July 1, 2009; accepted July 2, 2009.

From the Department of Pharmacology (R.G., R.C., A.B., I.A., M.V., L.O., J.T., E.D.), School of Medicine, Universidad Complutense, Madrid, Spain; Centro Nacional de Investigaciones Cardiovasculares (E.C., J.A.L.), Madrid, Spain; Department of Physiology, Montreal University (H.K.), Canada; and Hospital General Universitario Gregorio Marañón (F.A., J.A., A.P.), Madrid, Spain.

*Both authors contributed equally to this work.

Correspondence to Ricardo Caballero, Department of Pharmacology, School of Medicine, Universidad Complutense, 28040 Madrid, Spain. E-mail rcaballero@med.ucm.es

© 2009 American Heart Association, Inc.

Circulation Research is available at <http://circres.ahajournals.org>

DOI: 10.1161/CIRCRESAHA.109.197558

Non-standard Abbreviations and Acronyms	
τ_o	open-time constant
τ_c	closed-time constant
AP	action potential
APD	action potential duration
cAF	chronic atrial fibrillation
CHO	Chinese hamster ovary cells
DEANO	<i>N,N</i> -diethylamine-diazenolate-2-oxide
DTT	dithiothreitol
E_K	reversal potential of K^+
f_o	opening frequency
I_{K1}	cardiac inwardly rectifying K^+ current
I_{KACH}	acetylcholine-activated component of the inward rectifier current
I_{KATP}	ATP-sensitive K^+ current
$I_{Kir2.1}$	Kir2.1 current
Kir2.1Cyt	peptide of the Kir2.1 cytoplasmic region spanning residues 48 to 80
I_{NCX}	Na^+/Ca^{2+} exchange current
I-V	current-voltage
$[K^+]_o$	extracellular K^+ concentration
LC-MS	liquid chromatography/tandem mass spectrometry
NO	nitric oxide
ODQ	1 <i>H</i> -[1,2,4]oxadiazolo[4,3- <i>a</i>]quinoxalin-1-one
P_o	open probability
RMP	resting membrane potential
sGC	soluble guanylyl cyclase
SIM	single ion monitoring
SNAP	(\pm)- <i>S</i> -nitroso- <i>N</i> -acetylpenicillamine
SR	sinus rhythm
WT	wild type

scribed that NO, at physiological myocardial concentrations, hyperpolarizes RMP and shortens AP duration (APD) measured at 50% and 90% of repolarization in mouse isolated atria.⁸ NO-induced shortening appeared in the range of membrane potentials negative to -40 mV, which corresponds to the phase of repolarization where the contribution of I_{K1} is most significant, suggesting that NO regulates I_{K1} .

Thus, in this study, the effects of NO on human atrial I_{K1} and Kir2.1 channels, as well as the mechanisms involved in these actions, have been analyzed. The results demonstrated that NO regulates cardiac excitability by the selective *S*-nitrosylation of Cys76 of the Kir2.1 protein.

Methods

The study was approved by the Investigation Committee of the Hospital Universitario Gregorio Marañón (CNIC-13) and conforms to the principles outlined in the Declaration of Helsinki. Each patient gave written informed consent. Myocytes were enzymatically isolated from right atrial appendages obtained from patients in sinus rhythm (SR) undergoing cardiac surgery.⁸

Human Kir2.1 wild-type (WT) and mutated channels were transiently transfected in CHO cells.^{8,9} The NO donors (\pm)-*S*-nitroso-*N*-acetylpenicillamine (SNAP) and *N,N*-diethylamine-diazenolate-2-oxide (DEANO) were initially dissolved in ethanol and water,

respectively and the NO-saturated solution was obtained as described.^{8,9} Macroscopic and single-channel currents were recorded using the whole-cell and cell-attached patch-clamp configurations, respectively.

The *S*-nitrosylation of a synthetic peptide spanning sequence 48-VKKDGHCVQFINVGEKGRYLDIFTTCVDIR-80 from the cytoplasmic tail of Kir2.1 was determined by liquid chromatography/tandem mass spectrometry (LC-MS). Single ion monitoring (SIM) experiments were performed for the masses corresponding to the unmodified and nitrosylated-tryptic peptides. Detection of *S*-nitrosylated Kir2.1 in mouse ventricular and human atrial samples was performed using the biotin-switch assay, followed by Western blot.^{8,9}

Results are expressed as mean \pm SEM. Paired or unpaired *t* test or 1-way ANOVA followed by Newman-Keuls test were used to assess statistical significance where appropriate. A value of $P < 0.05$ was considered significant.

An expanded Methods section is available in the Online Data Supplement at <http://circres.ahajournals.org>.

Results

NO Increases Human Atrial I_{K1}

Figure 1 shows original recordings (Figure 1A) and mean current-voltage (I-V) relationships (Figure 1B) for I_{K1} obtained in isolated human atrial myocytes by applying a voltage ramp from -100 to -10 mV in the absence and presence of the NO donor SNAP (200 μ mol/L). SNAP increased both inward ($23.6 \pm 5.5\%$ at -100 mV) and outward I_{K1} ($67.9 \pm 12.4\%$ at -10 mV) ($n=8$, $P < 0.05$ versus control). These experiments were performed in the presence of atropine (1 μ mol/L) to block the acetylcholine-activated component of the inward rectifier current (I_{KACH}). Under these conditions, activation of the ATP-sensitive K^+ current (I_{KATP}) is very unlikely because intracellular solution was supplemented with ATP. Nevertheless, we analyzed the effects of SNAP in the presence of glibenclamide (10 μ mol/L), a selective I_{KATP} blocker. Figure 1E demonstrates that even in the presence of glibenclamide, SNAP increased the I_{K1} measured at -100 mV by $18.2 \pm 2.8\%$ ($n=4$, $P < 0.05$). To further isolate the effects of SNAP on I_{K1} , we used $BaCl_2$ (100 μ mol/L), a selective blocker of I_{K1} in the presence of atropine and glibenclamide. Application of SNAP increased the Ba^{2+} -sensitive current, which displayed strong inward rectification, without modifying the Ba^{2+} -insensitive current, adding strong support to the hypothesis that the current increased by SNAP is I_{K1} (Figure 1C and 1E). However, as can be observed in the inset of Figure 1C the SNAP-increased Ba^{2+} -sensitive current seemed to display less inward rectification than I_{K1} . Moreover, the Na^+/Ca^{2+} exchange current (I_{NCX}) can also be activated over the voltage range tested. Therefore we analyzed the effects of SNAP on I_{NCX} . Extracellular solution (containing atropine and glibenclamide) was supplemented with ouabain (10 μ mol/L) to inhibit the Na^+/K^+ ATPase and I_{NCX} was measured as the difference between the current recorded in the presence of extracellular Ca^{2+} and that recorded in the presence of 5 mmol/L Ni^{2+} (0 mmol/L Ca^{2+}). Online Figure I demonstrates that SNAP did not modify the I_{NCX} .

Next, the effects of SNAP on APs recorded in isolated human atrial myocytes were analyzed. As shown in Figure 1D, application of SNAP (in the presence of atropine and glibenclamide) slightly but significantly hyperpolarized the RMP (from -69.8 ± 2.7 to -72.8 ± 3.2 mV, $n=4$, $P < 0.05$)

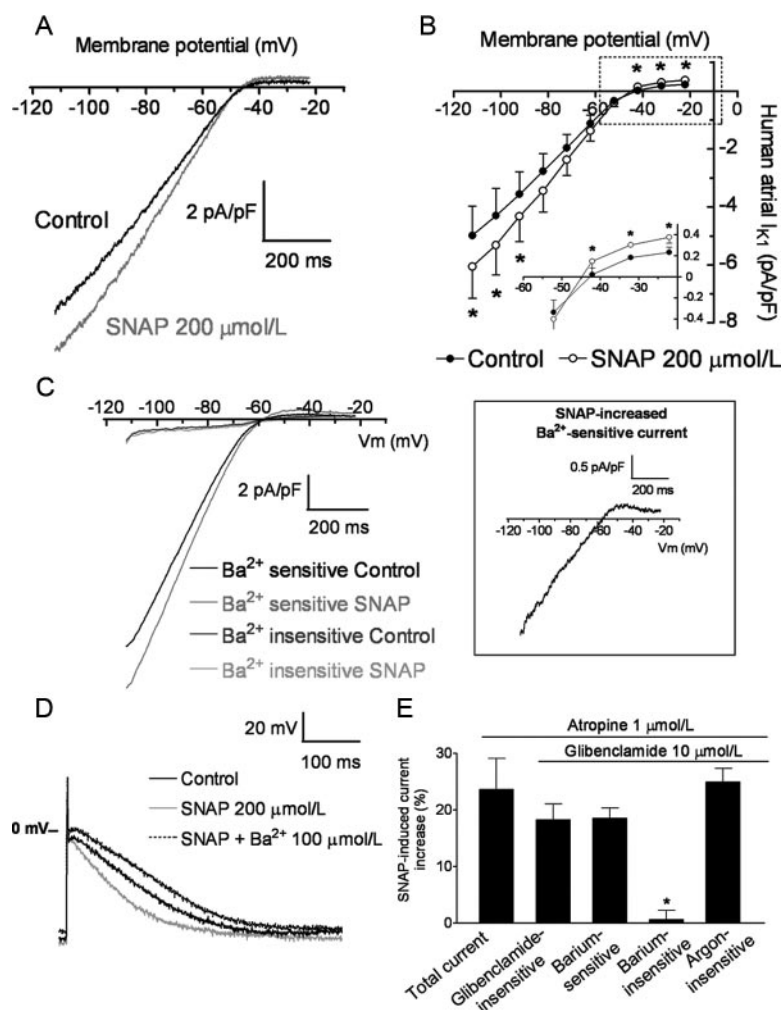


Figure 1. SNAP increases human atrial I_{K1} . A, Voltage ramp (800 ms) from -100 to -10 mV in the absence and presence of $200 \mu\text{mol/L}$ SNAP. B, I-V curves for human atrial I_{K1} in the absence and presence of SNAP. The inset shows data at potentials positive to E_K in an expanded scale. C, Representative Ba^{2+} -sensitive and Ba^{2+} -insensitive currents recorded before and after application of SNAP by applying a voltage ramp (800 ms) from -100 to -10 mV. The inset (right box) shows the SNAP-increased Ba^{2+} -sensitive current. In panels A to C, the voltage is adjusted to the liquid junction potential of 12.1 mV. D, AP recorded in a human atrial myocyte in control conditions ($1 \mu\text{mol/L}$ atropine and $10 \mu\text{mol/L}$ glibenclamide), in the presence of SNAP and after perfusion of SNAP and Ba^{2+} . E, Percentage of I_{K1} SNAP-induced increase at -100 mV under different experimental conditions. Each point/column represents the mean \pm SEM of ≥ 4 experiments. $*P < 0.05$ vs control.

and shortened the APD_{90} (from 227 ± 12 to 173 ± 16 ms, $P < 0.05$). Further addition of Ba^{2+} not only completely reversed the effect of SNAP but also increased the APD_{90} to 286 ± 46 ms and depolarized the RMP (-64.9 ± 1.3 mV, $P < 0.05$). These results suggest that the NO effects on I_{K1} have a significant impact on the shape of human atrial AP.

NO Increases Kir2.1 Currents

Because human I_{K1} is mainly carried by Kir2.1 channels, we studied the effects of NO on Kir2.1 currents ($I_{\text{Kir}2.1}$) recorded in transiently transfected CHO cells. Figure 2A shows $I_{\text{Kir}2.1}$ recorded by applying 250-ms pulses from -60 mV to potentials ranging -120 and $+20$ mV in the absence and presence of $200 \mu\text{mol/L}$ SNAP. SNAP increased $I_{\text{Kir}2.1}$ at voltages negative ($20.9 \pm 5.9\%$ at -120 mV) and positive to E_K ($51.7 \pm 11.1\%$ at -50 mV) (Figure 2A and 2B) ($n = 7$, $P < 0.05$). The SNAP-induced increase was completely reversible on washout. The time course of the NO concentrations in the cell chamber after beginning the SNAP perfusion was measured using a potentiometric NO sensor (see Online Data Supplement).^{8,9} NO concentration reached a maximum within 4 to 6 minutes (182 ± 35 nmol/L with SNAP $200 \mu\text{mol/L}$, $n = 7$) and remained stable during SNAP perfusion (10 to 12 minutes), decreasing to basal levels after perfusion with SNAP-free solution. In Figure 2C, the $I_{\text{Kir}2.1}$

increase measured at the end of pulses to -120 mV was represented as a function of the SNAP concentration. At concentrations higher than $200 \mu\text{mol/L}$ SNAP induced a similar amount of increase. The Hill equation was used to fit the concentration dependence of the increase, and the EC_{50} and the maximum effect obtained were $82.8 \pm 3.6 \mu\text{mol/L}$ ($n_H = 3.1 \pm 0.8$) and $21.5 \pm 0.5\%$, respectively. When the increase was plotted as a function of the released NO, the EC_{50} was 75.4 ± 3.4 nmol/L ($n_H = 3.1 \pm 0.8$) (Figure 2D).

The effects of another NO donor ($3 \mu\text{mol/L}$ DEANO) and an NO-saturated solution, which yielded NO concentrations of 247 ± 23 and 205 ± 13 nmol/L, respectively (Figure 3A and 3B), were also studied. To prepare the NO-saturated solution, the external solution was bubbled with argon (Ar) for 20 to 30 minutes in a gas-washing bottle obtaining an O_2 -free solution and, then, with NO for 30 minutes (see Online Data Supplement). Control data were obtained in the presence of the O_2 -free Ar-saturated solution.^{8,9} DEANO (Figure 3C) and the NO solution (Figure 3D) also significantly increased inward $I_{\text{Kir}2.1}$ by $17.3 \pm 2.5\%$ ($n = 7$) and $17.7 \pm 1.4\%$ ($n = 4$) at -120 mV, respectively, and outward $I_{\text{Kir}2.1}$ by $52.3 \pm 12.0\%$ and $60.3 \pm 2.2\%$ at -50 mV, respectively. These effects were not different from those obtained with SNAP at concentrations that release equivalent levels of NO and indicated that, in all cases, the $I_{\text{Kir}2.1}$ increase was exclusively attributable to NO.

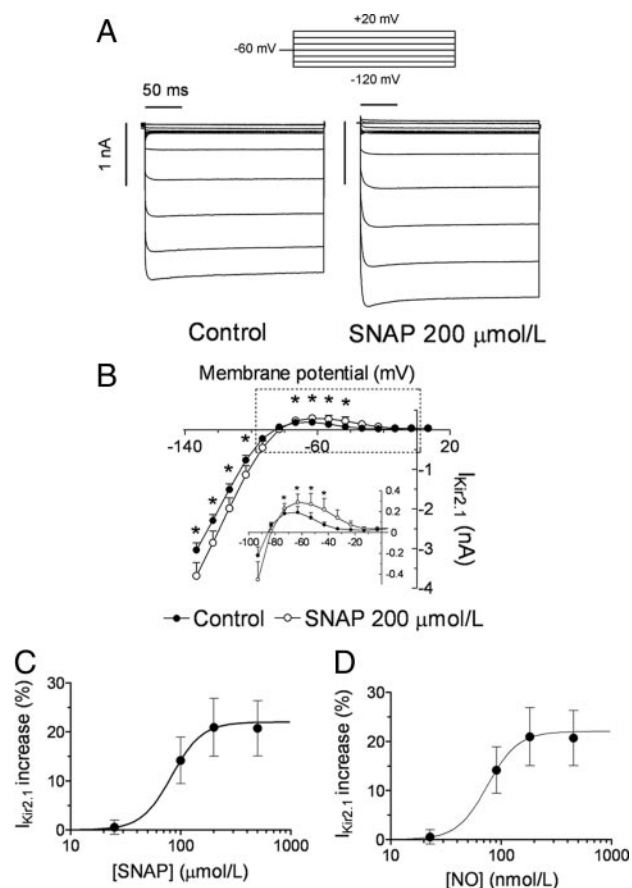


Figure 2. SNAP increases $I_{Kir2.1}$. A, $I_{Kir2.1}$ traces recorded by applying 250-ms pulses from a holding potential of -60 mV to potentials ranging -120 and $+20$ mV in the absence and presence of $200 \mu\text{mol/L}$ SNAP. B, I-V curves for currents measured at the end of the pulses. The inset shows data at potentials positive to E_K in an expanded scale. Percentage of $I_{Kir2.1}$ increase at -120 mV as a function of SNAP (C) and the released NO (D) concentrations. Each point represents the mean \pm SEM of >7 experiments. $*P < 0.05$ vs control.

Because it has been demonstrated that hypoxia increases mouse cardiac I_{K1} ,¹⁰ we analyzed the effects of SNAP when added to an O_2 -free Ar-saturated solution on human atrial I_{K1} . Control data were obtained in the presence of an O_2 -free Ar-saturated solution. Figure 1E shows that SNAP increased the Ar-insensitive current at -100 mV by $24.9 \pm 2.4\%$ ($P < 0.05$, $n = 4$). Therefore, increasing effects produced by NO were apparent even in hypoxic conditions.

NO-Induced Increase Is Not Dependent on the Extracellular K^+ Concentration

Kir2.1 channel conductance and inward rectification are strongly dependent on the extracellular K^+ concentration ($[K^+]_o$).^{1,2} Therefore, we analyzed whether the NO-induced increase was dependent on the $[K^+]_o$, by comparing the effects of SNAP on $I_{Kir2.1}$ recorded at 1 and 10 mmol/L $[K^+]_o$ (Figure 4) with those observed at 4 mmol/L. Progressive increase of $[K^+]_o$ produced an increase in inward and outward $I_{Kir2.1}$ and a rightward shift in the E_K (Figure 4A). Figure 4C and 4D shows I-V curves in the absence and presence of SNAP at 1 and 10 mmol/L $[K^+]_o$, respectively.

At 1 mmol/L $[K^+]_o$, $I_{Kir2.1}$ was recorded by applying 250-ms pulses from -60 mV to potentials ranging -150 and -10 mV, because at this $[K^+]_o$, the E_K was shifted to -127.9 ± 1.3 mV. SNAP increased both inward and outward currents by $22.2 \pm 2.6\%$ and $46.4 \pm 7.8\%$ at -150 mV and -80 mV, respectively ($n = 7$). At 10 mmol/L ($E_K = -68.1 \pm 2.6$ mV), currents were recorded by applying 250-ms pulses from -60 mV to potentials ranging from -120 to $+20$ mV, and SNAP also increased $I_{Kir2.1}$ at potentials negative ($20.0 \pm 7.1\%$ at -100 mV) and positive ($59.9 \pm 7.9\%$ at -30 mV) to the E_K ($n = 5$). Finally, as shown in Figure 4B, SNAP did not modify the E_K at any of the $[K^+]_o$ tested.

NO Increases Open Probability of Kir2.1 Channels

The effects of NO on unitary Kir2.1 currents were also analyzed. Figure 5A shows single-channel recordings in a CHO cell expressing Kir2.1 channels by applying 1-second pulses to -80 mV from a holding potential of 0 mV in the absence and presence of $200 \mu\text{mol/L}$ SNAP. Kir2.1 channel activity was characterized by few and long events leading to a mean open probability (P_o) of 0.18 ± 0.01 and an opening frequency (f_o) of 2.6 ± 0.1 Hz (Figure 5D and 5E) ($n = 6$). Amplitude of unitary currents in control conditions and in the presence of $200 \mu\text{mol/L}$ SNAP were calculated for each experiment from a Gaussian distribution fit to amplitude histograms that were constructed by plotting amplitude data as a function of the number of events per bin (Online Figure II). SNAP did not modify unitary current amplitude (Figure 5F) but induced a significant change in channel gating characterized by a marked increase in the frequency of events, which appeared as brief channel openings (Figure 5A). Open- and closed-time constants (τ_o and τ_c) were calculated for each experiment from the Gaussian distribution fit to dwell-time histograms that were constructed by plotting dwell-time data as a function of the number of events per bin. Figure 5B and C show dwell-time histograms constructed from pooled experiments. SNAP decreased τ_o from 49.4 ± 16.5 to 27.0 ± 3.9 ms and τ_c from 275.5 ± 47.5 to 154.1 ± 64.8 ms ($P < 0.05$) and increased the f_o (6.9 ± 0.2 Hz; $P < 0.01$) (Figure 5E), which eventually led to an increase in the P_o (0.26 ± 0.01 ; $P < 0.05$) (Figure 5D).

Cys76 Is Responsible for the NO-Induced Increase of Kir2.1

The next step was to elucidate the signaling pathway responsible for the NO-induced $I_{Kir2.1}$ increase. The activation of soluble guanylyl cyclase (sGC)/cGMP/protein kinase G signaling pathway is the most common mechanism implicated in NO effects.⁷ For testing whether this pathway was responsible for the effects, $1H$ -[1,2,4]oxadiazolo[4,3-*a*]quinoxalin-1-one (ODQ), a selective inhibitor of sGC was used. In the presence of ODQ ($50 \mu\text{mol/L}$), SNAP ($200 \mu\text{mol/L}$) increased $I_{Kir2.1}$ to a similar extent ($19.2 \pm 6.9\%$ at -120 mV) as that produced by SNAP alone ($n = 6$, $P > 0.05$), which discards the involvement of the sGC/cGMP/protein kinase G pathway in the effects.

Posttranslational modifications induced by NO have emerged as important mechanisms by which NO can regulate protein function. These modifications include Cys

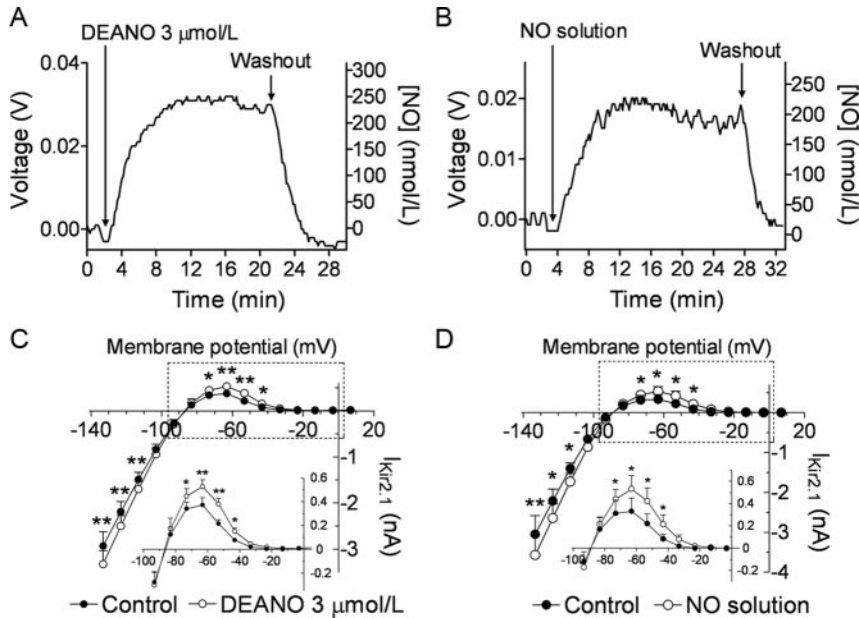


Figure 3. DEANO and an NO solution also increase $I_{Kir2.1}$. NO concentrations yielded before and after perfusion of 3 μmol/L DEANO (A) and an NO-saturated solution (B). I-V curves under control conditions and in the presence of DEANO (C) or the NO solution (D). The insets show data at potentials positive to E_K in an expanded scale. * $P < 0.05$ and ** $P < 0.01$ vs control. Each point represents the mean \pm SEM of > 4 experiments.

S-nitrosylation and Tyr nitration, which are highly dependent on the cellular redox state.¹¹ To determine whether some of these modifications could be responsible for the NO-induced increase of $I_{Kir2.1}$, the effects of SNAP in the presence of the reducing agent dithiothreitol (DTT) (5 mmol/L) were studied. DTT per se did not modify $I_{Kir2.1}$ (Figure 6A) but completely prevented the increase induced by SNAP. Identical results were obtained on human atrial I_{K1} (Figure 6B). These results suggested the implication of posttranslational modifications in the effects of NO on $I_{Kir2.1}$ and I_{K1} . The reversibility of the NO-induced increase was in concordance with the characteristic lability of the S-nitrosylation of Cys residues, suggesting that this modification was mediating the effects of NO on Kir2.1 channels. To determine the involvement of 1 or some of the 13 Cys of the Kir2.1 channel, site-directed mutagenesis experiments were performed. First, we tried to evaluate the effects of SNAP on a Kir2.1 channel in which all the Cys (with the exception of Cys122 and Cys154, which are

essential for proper channel folding),¹² were substituted. However, this “Cys-free” mutant did not generate functional channels. Next, we analyzed the effects of SNAP on IRK1J, a Kir2.1 channel in which 6 Cys residues (C54V, C76V, C89I, C101L, C149F, and C169V) were mutated simultaneously.¹³ In IRK1J channels, SNAP failed to modify the current, indicating the implication of 1 or some of these Cys in the NO-induced increase (Figure 6C). To determine which of these Cys was involved, the effects of SNAP on Kir2.1 channels with individual mutations were studied. When possible, substitution of Cys by Ser was chosen because the replacement of Cys-sulfur by the Ser-oxygen keeps the hydrogen bonding capability in most of the cases and, thus, the essential features of the channel (C54S, C101S, C149S).¹² Other substitutions were introduced in those channels in which Ser substitution induced dramatic changes in channel properties (C76L, C76V, C89G, C169A).¹² The characteristics of the currents generated by all these mutants were

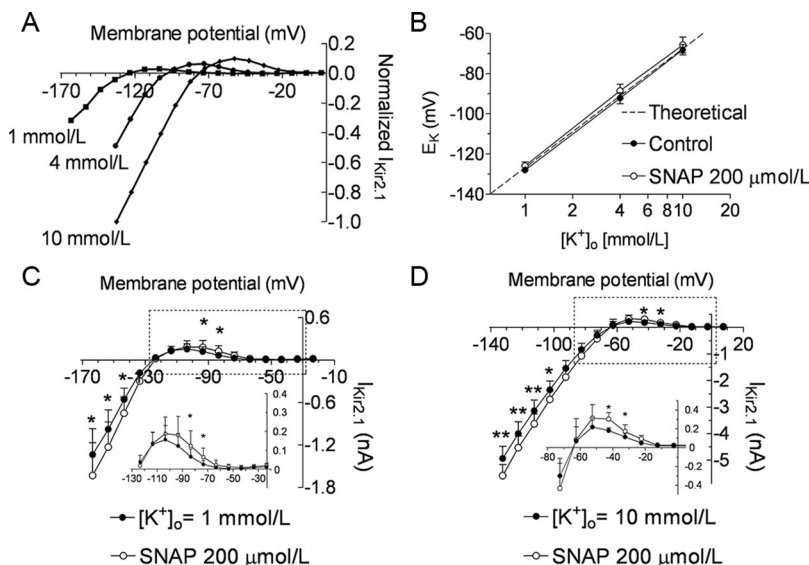


Figure 4. NO-induced increase of $I_{Kir2.1}$ is not dependent on $[K^+]_o$. A, Normalized I-V curves for $I_{Kir2.1}$ recorded in CHO cells perfused with an external solution containing 1, 4, or 10 mmol/L $[K^+]_o$. B, E_K values in the absence and presence of 200 μmol/L SNAP and the theoretical values obtained from the Nernst equation plotted as a function of the $[K^+]_o$. I-V curves under control conditions and in the presence of SNAP at 1 mmol/L (C) or 10 mmol/L $[K^+]_o$ (D). The insets show data at potentials positive to E_K in an expanded scale. * $P < 0.05$ and ** $P < 0.01$ vs control. Each point represents the mean \pm SEM of > 5 experiments.

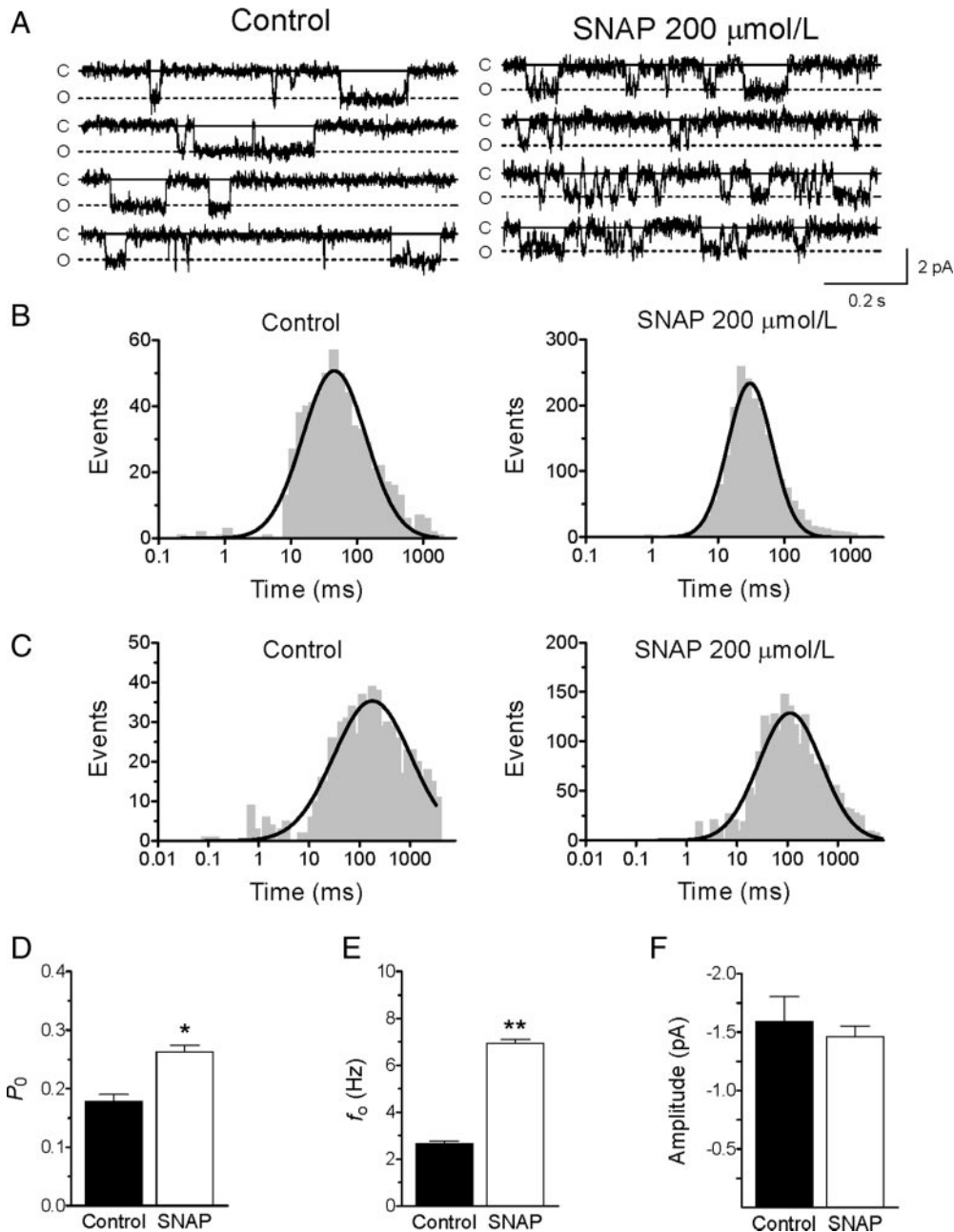


Figure 5. NO increases P_0 and f_0 but decreases τ_0 of Kir2.1 channels. A, Single-channel recordings in a CHO cell under control conditions and after perfusion with 200 μmol/L SNAP. Closed and open channel levels are indicated by C and O, respectively. Dwell-time histograms of open (B) and closed (C) times of single Kir2.1 channels recorded in the absence and presence of SNAP (10 bins/decade). Continuous lines represent the fit of a Gaussian distribution to the data. Histograms were obtained by pooling data from 6 experiments. P_0 (D), f_0 (E), and unitary current amplitude (F) in the absence and presence of SNAP. Each column represents the mean \pm SEM of 6 experiments. * $P < 0.05$ and ** $P < 0.01$ vs control.

similar to those of the Kir2.1 WT. SNAP also increased inward and outward currents generated by the mutants, with the exception of C76L and C76V channels, in which SNAP failed to increase $I_{Kir2.1}$ both at potentials negative and positive to E_K (Figure 6D and 6E). The percentage of change at -120 mV for all the constructs is summarized in Figure 6E. These results indicated that Cys76 is critical for the $I_{Kir2.1}$ increase induced by NO. Finally, we studied the effects of SNAP on cells cotransfected with both WT and C76L Kir2.1 channels. Under these conditions, the NO donor failed to increase inward and outward $I_{Kir2.1}$ (Figure 6E).

Residue Cys76 Is Nitrosylated in a Kir2.1 Cytoplasmic Peptide

The thiol group of Cys76 is located in the vicinity of acid and basic residues that could act as catalysts for *S*-nitrosylation.¹¹ For testing whether the primary sequence of the protein determines the specific *S*-nitrosylation of Cys76, a peptide of the Kir2.1 cytoplasmic region spanning residues 48 to 80 (Kir2.1Cyt), which contained Cys54 and Cys76, was synthesized (Figure 7A). Kir2.1Cyt was treated with SNAP and then trypsin-digested to yield 2 peptides (DGHCNVQFINVGEK and YLADIFTTCVDIR) containing the Cys54 and Cys76

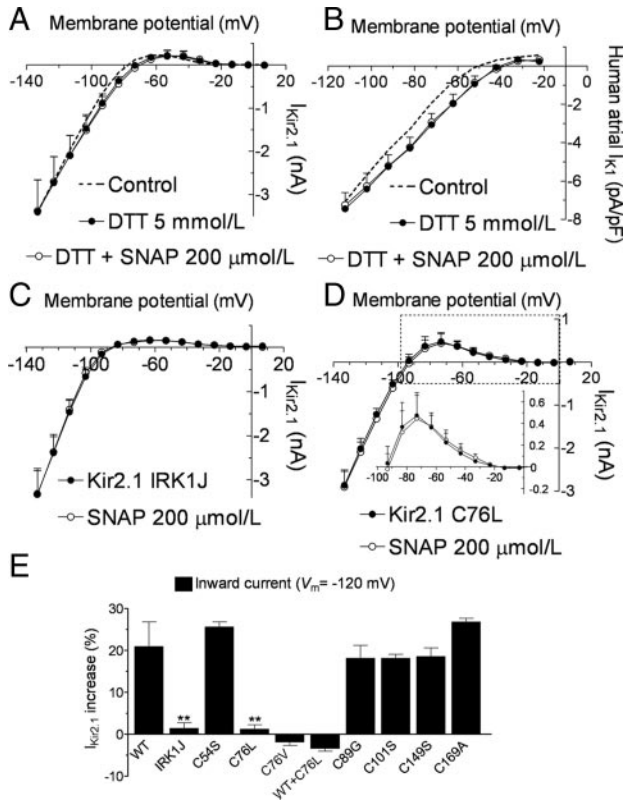


Figure 6. NO-induced increase is dependent on the cellular redox state and is determined by Cys76. I-V curves for $I_{Kir2.1}$ (A) and human atrial I_{K1} (B) in the absence (control, dashed line) and presence of DTT (5 mmol/L) alone or plus SNAP (200 μ mol/L). I-V curves for currents recorded in CHO cells expressing IRK1J (C) or C76L (D) Kir2.1 channels in the absence and presence of SNAP. E, SNAP-induced change on the current recorded at -120 mV in CHO cells expressing WT or mutant Kir2.1 channels. ** $P < 0.01$ vs WT. Each point/column represents the mean \pm SEM of > 4 experiments.

residues, respectively. SIM experiments were performed by LC-MS for masses at m/z 780.3 and 794.8 Da (unmodified and nitrosylated Cys54, respectively), and at m/z 765.3 and 779.8 Da (unmodified and nitrosylated Cys76, respectively), corresponding to doubly charged Kir2.1-derived tryptic peptides (Figure 7). The SIM analysis detected both unmodified peptides containing the Cys54 or Cys76 residues but only detected the ion at m/z 779.8 Da, corresponding to the nitrosylated Cys76 peptide (Figure 7B), as revealed by comprehensive analysis of fragmentation spectra (Figure 7C). No nitrosylated Cys54 peptide was found in the expected retention time (Figure 7B, arrow). These results suggest that the primary sequence surrounding Cys76 promotes its selective S-nitrosylation.

S-Nitrosylation of Kir2.1 in Response to Changes in Myocardial NO Concentrations

To test the effects of changes in myocardial NO concentrations on the S-nitrosylation level of Kir2.1 channels we followed 2 experimental strategies. First, we tested the effects of the increase of the NO concentration in mouse ventricular samples. Putative Kir2.1 S-nitrosylated protein was labeled with biotin and detected with streptavidin-peroxidase follow-

ing the biotin-switch assay.^{8,9} Representative Western blot demonstrated that in mouse ventricle treatment with 200 μ mol/L SNAP increased the S-nitrosylation of several proteins including Kir2.1, which was identified by a parallel Western blot with Kir2.1 antibodies (Online Figure III).

Secondly, we tested the effects of a decrease in the myocardial NO concentration. Oxidative stress in the setting of chronic atrial fibrillation (cAF) markedly reduces atrial NO concentrations.¹⁴ Preliminary analysis of the S-nitrosylation level of Kir2.1 was done by developing a biotin-switch assay in right atrial appendages obtained from patients in SR and cAF. Figure 8A and 8B suggests that S-nitrosylated Kir2.1 proteins were less abundant in samples from cAF patients even when Kir2.1 proteins are expected to be more abundant in those samples.¹⁵

Discussion

In the present report, we demonstrate that NO, at physiological concentrations, increases $I_{Kir2.1}$ by augmenting the open probability of the channel as a result of the S-nitrosylation of Cys76. The findings provide a deeper insight into the modulation of cardiac I_{K1} and describe, for the first time, an important mechanism by which NO participates in the regulation of cardiac RMP and in shaping APs.

NO Increases $I_{Kir2.1}$

Two NO donors (SNAP and DEANO) and an NO-saturated solution induced a concentration-dependent increase of both inward and outward $I_{Kir2.1}$. The fact that the effects were quantitatively and qualitatively similar when using the NO solution and the donors strongly suggests that the increase of $I_{Kir2.1}$ is exclusively mediated by NO and does not involve other NO-independent mechanisms.

It is well established that Kir2.1 channel conductance and inward rectification are strongly dependent on the $[K^+]_o$.^{1,2} Indeed, inward rectifier channel blockade induced by Mg^{2+} or polyamines is modulated by changes in the $[K^+]_o$.^{1,2} Our experiments demonstrated that NO-induced increase was apparent at low and high $[K^+]_o$, suggesting that the mechanism responsible for the effect does not interfere with the binding site of K^+ to the channel.¹ Moreover, we also showed that NO did not modify the E_K , indicating that it did not change the K^+ selectivity of the channel.

Single-channel experiments demonstrated that NO did not modify the unitary current amplitude, but increased the P_o as a consequence of a ≈ 3 -fold increase of the f_o in spite of a significant reduction in the τ_o . These results clearly pointed to an effect of NO on the channel gating rather than an increase of the number of functional channels and suggest that NO facilitates the close-to-open transition and accelerates the channel closing kinetics.

Posttranslational Modifications Responsible for the NO-Induced Increase

Our results demonstrated that the effects of NO on $I_{Kir2.1}$ and I_{K1} are mediated by a posttranslational modification that depends on the redox state of the cell, because they were abolished by the reducing agent DTT. Among these modifications, S-nitrosylation of Cys residues is considered the most

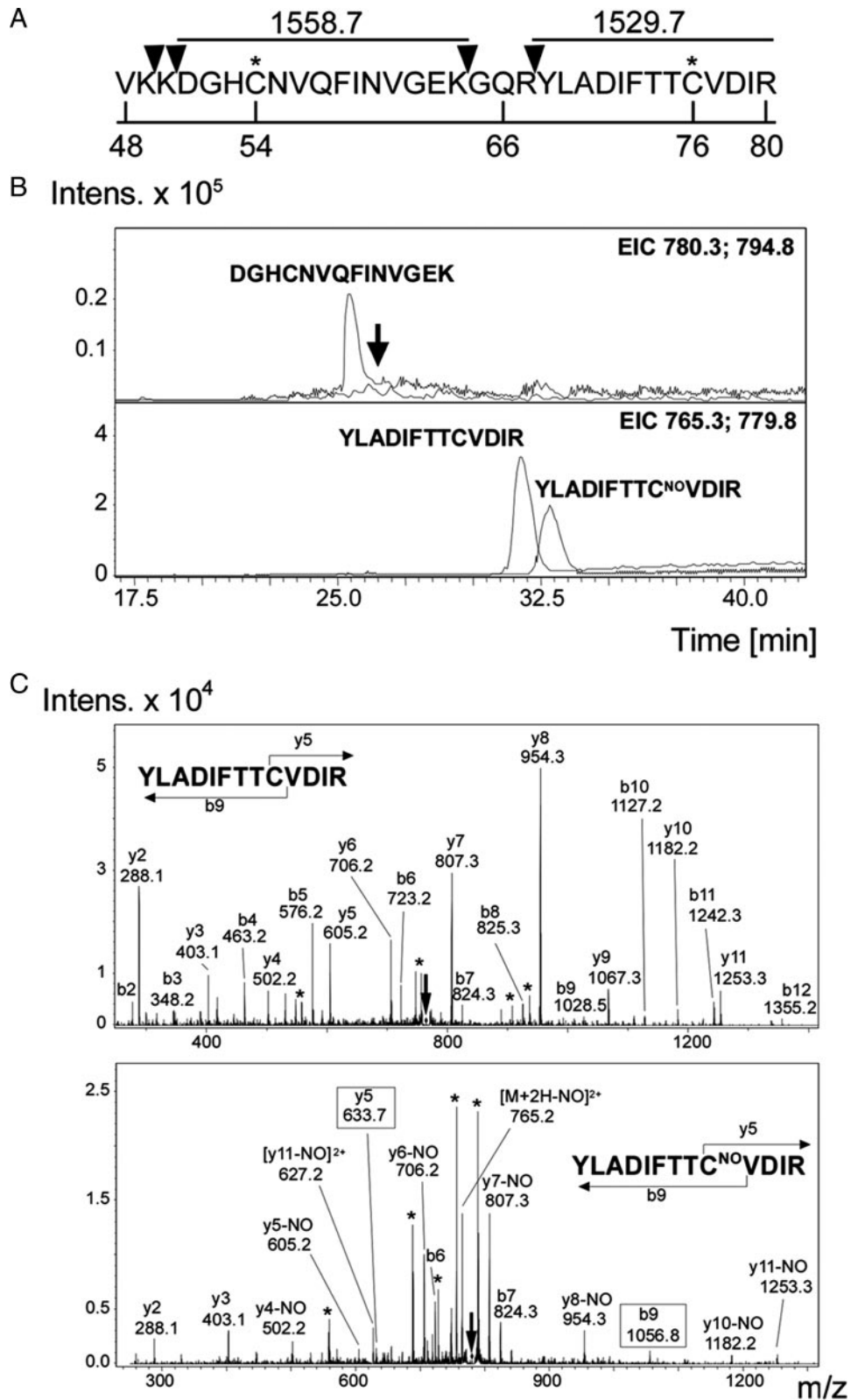


Figure 7. Characterization of the nitrosylation site in Kir2.1 peptide by LC-MS. A, Sequence of peptide Kir2.1Cyt (residues 48 to 80 from cytoplasmic tail) showing the potential trypsin cleavage sites (triangles) and the monoisotopic masses of the longer Kir2.1Cyt-derived tryptic peptides. B, SIM chromatograms for doubly charged Kir2.1-derived tryptic peptides masses at m/z 780.3 and 794.8 Da (unmodified and nitrosylated Cys54) (top) and at m/z 765.3 and 779.8 Da (unmodified and nitrosylated Cys76) (bottom). Black arrow indicates the expected retention time for nondetected Cys54 nitrosylated peptide. C, Fragmentation spectra from Cys76-unmodified (top) and Cys76-nitrosylated (bottom) Kir2.1 tryptic peptide. Diagram shows fragment ions corresponding to main fragmentation series (b-amino and y-carboxy). * indicates water loss; 2+, doubly charged fragments. Parental ion from each peptide is marked with an arrow. Numbered boxes indicate nitrosylation as revealed by both b and y series.

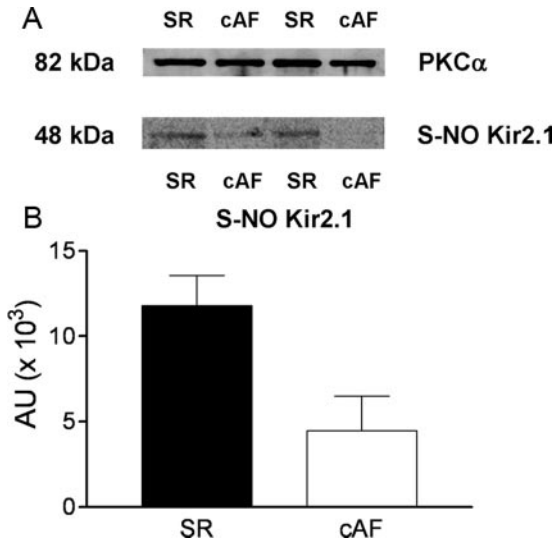


Figure 8. S-Nitrosylation of myocardial Kir2.1. A, Representative Western blots showing S-nitrosylated Kir2.1 in right atrial appendage obtained from patients in SR or cAF. Protein kinase C α (PKC α) (top) was used as a loading control. B, Densitometric analysis of the Western blots. Results are presented as the mean \pm SEM of 2 patients in each group.

important because of its high reactivity, occurrence at physiological conditions, and influence on many protein functions.¹¹ Our site-directed mutagenesis analysis demonstrated that NO increase of $I_{Kir2.1}$ was mediated by its specific and selective interaction with Cys76. Selective S-nitrosylation of one of many available Cys residues in a protein can be achieved through many mechanisms, including the existence of a favorable chemical context for reaction with NO.¹¹ This mechanism would involve the existence of an acid–base flanking consensus motif and electrostatic interactions with appropriately oriented aromatic amino acid side chains. This chemical context can be provided by adjacent residues in the primary sequence or just in the proximity in the 3D structure.¹¹ In this regard, in the primary sequence Cys76 is surrounded by 2 Asp (71 and 78) and 1 Arg (80), and it is preceded by an aromatic amino acid (Phe73) that could act as catalysts for S-nitrosylation. Furthermore, a Kir2.1 homology model based on the crystal structure of KirBac1.1¹⁶ shows that in the 3D structure the thiol group of Cys76 is surrounded at less than 6 Å by the carboxyl groups of those Asp. SIM analysis of the Kir2.1Cyt peptide demonstrated the selective S-nitrosylation of Cys76, and not of Cys54, suggesting that acid–base interactions with neighboring group in the primary sequence and the close presence of the aromatic moiety determine the selective S-nitrosylation of Cys76. It is interesting to note that Cys76 belongs to a common highly conserved motif (74-TTxxDxxWR-83) located in the N terminus in close proximity to the first transmembrane segment in the Kir superfamily.¹² Some residues of this mildly hydrophobic area (Q region) are located within an amphipathic α -helical domain termed “slide helix” that runs parallel to the inner leaflet of the plasma membrane.¹⁷ The slide helix is organized so that hydrophilic and hydrophobic residues are located in opposite sides with Cys76 centered on the hydrophobic face.¹² It must be considered that local

hydrophobicity might also promote specific S-nitrosylation of Cys that belong to protein domains that reside in a juxtamembrane zone.¹¹ Therefore, the hydrophobic environment in which Cys76 is involved could also contribute to its specific S-nitrosylation.

The slide helix has been proposed to be essential for proper channel gating.¹⁶ In fact, several mutations causing Andersen–Tawil syndrome affect residues located in this region.¹⁷ Furthermore, Cys76 has already been reported to be involved in the gating and conduction properties of Kir2.1 channels. Indeed, its mutation to charged/polar amino acids abolishes channel activity because of the destabilization of the open state.¹²

The NO effects were only apparent in Kir2.1 channels in which the 4 subunits contain the Cys76 and not in WT+C76L channels. This is consistent with the observation that the 4 subunits in the Kir channels function in a highly cooperative way.¹⁸ Moreover, Cys76 is highly conserved in the Kir2 family, also being present in Kir2.2 (Cys75) and Kir2.3 (Cys50) channels. In fact, both $I_{Kir2.2}$ and $I_{Kir2.3}$ were also increased by SNAP in a similar extent than $I_{Kir2.1}$ (Online Figures IV and V). This could explain why the NO-induced increase was also observed in the human atrial I_{K1} , where the relative contribution of Kir2.2 and Kir2.3 seems to be even greater than that of Kir2.1.⁴

Potential Physiological Significance

The results obtained in human atrial myocytes strongly suggest that the current increased by NO is I_{K1} . However, the SNAP-increased Ba²⁺-sensitive current seemed to display less inward rectification than I_{K1} , which could suggest the involvement of other inward rectifying currents. Under our experimental conditions (in the presence of glibenclamide and atropine), activation of I_{KATP} and I_{KACH} is very unlikely; however, we cannot rule out that NO increases other currents, particularly the constitutively active I_{KACH} , which is not inhibited by atropine.

Physiological myocardial NO levels display rapid fluctuations within the cardiac cycle, ranging from 0.26 μ mol/L during the systole to 0.93 μ mol/L during the diastole.¹⁹ The NO concentrations used in this study (\approx 0.2 μ mol/L) are in the lower range of cardiac NO concentrations, indicating that Kir2.1 channels exhibit a high affinity for NO. Many cardiovascular diseases are accompanied by significant changes in the myocardial NO production and/or bioavailability.⁷ For instance, a decrease in cAF¹⁴ and an increase during early ischemia and early reperfusion have been described.⁷ Our data suggest that in those diseases in which the NO concentration decreases, Kir2.1 channels would be less S-nitrosylated, an effect that, in turn, would decrease the I_{K1} . The contrary would be expected in those cardiovascular diseases in which myocardial NO markedly increases. Preliminary support to this hypothesis was obtained from the biotin-switch assay performed in a reduced number of samples of right atrial appendages obtained from SR and cAF patients. Further confirmation of these results would imply that the decrease in atrial NO concentrations will decrease the I_{K1} . However, it has been demonstrated that cAF increases the Kir2.1 expression level and the I_{K1} density.¹⁵ Thus, it

seems that in cAF the regulation of the expression level of Kir2.1 proteins and their posttranslational modification by S-nitrosylation operate in opposite directions. The putative role of the decrease in atrial NO concentrations in promoting or preventing the arrhythmia merits further detailed analysis.

I_{K1} plays a key role in cardiac electrophysiology by stabilizing the RMP and shaping the initial and the final phase of the atrial and ventricular AP.¹ Therefore, modulation of I_{K1} would have profound effects on cardiac excitability and arrhythmogenesis.² Conduction of the cardiac impulses depends on active and passive membrane properties. The slight hyperpolarization of the RMP produced by NO would influence both membrane properties because it would simultaneously increase the voltage-dependent Na^+ channel availability, decrease the resting membrane resistance, and impair the approach toward threshold potentials. The first effect would tend to increase, the other 2 to reduce cardiac excitability and conduction velocity. Furthermore, the strong outward component of the I_{K1} during repolarization rapidly restores the membrane potential to resting values. The increase of the I_{K1} outward component is probably responsible for the marked shortening of the final phase of AP repolarization produced by NO in mouse⁸ and human atria. This shortening would critically influence the refractory period. Moreover, the importance of I_{K1} in the establishment of a fast and stable reentry of a rotor has been demonstrated.⁶ The prediction is that I_{K1} helps to abbreviate the APD near the center of rotation (core); in addition, I_{K1} is also essential in maintaining the stability of these rotors.^{2,6}

Therefore, it can be concluded that the I_{K1} increase produced by the specific S-nitrosylation of Cys76 of Kir2.1 channels represents an important mechanism by which NO participates in the control of cardiac excitability under physiological conditions. Furthermore, this redox-related modulation is attributable to an increase in the opening frequency of Kir2.1 channels that exhibit an unexpected high affinity for this gaseous mediator.

Acknowledgments

We thank Dr Antonio Rodríguez Artalejo for his helpful suggestions.

Sources of Funding

Supported by Ministerio de Educación y Ciencia (SAF2005-04609, SAF2008-04903); Ministerio de Sanidad y Consumo; Instituto de Salud Carlos III (Red HERACLES RD06/0009 and PI080665); Fundación LILLY; and Centro Nacional de Investigaciones Cardiovasculares (CNIC-13). R.G. is a fellow of Comunidad Autónoma de Madrid.

Disclosures

None.

References

- Lopatin AN, Nichols CG. Inward rectifiers in the heart: an update on I_{K1} . *J Mol Cell Cardiol*. 2001;33:625–638.
- Dhamoon AS, Jalife J. The inward rectifier current I_{K1} controls cardiac excitability and is involved in arrhythmogenesis. *Heart Rhythm*. 2005;2:316–324.
- Wang Z, Yue L, White M, Pelletier G, Nattel S. Differential distribution of inward rectifier potassium channel transcripts in human atrium versus ventricle. *Circulation*. 1998;98:2422–2428.
- Gaborit N, Le Bouter S, Szuts V, Varro A, Escande D, Nattel S, Demolombe S. Regional and tissue specific transcript signatures of ion channel genes in the non-diseased human heart. *J Physiol*. 2007;582:675–693.
- Morita H, Wu J, Zipes DP. The QT syndromes: long and short. *Lancet*. 2008;372:750–763.
- Noujaim SF, Pandit SV, Berenfeld O, Vikstrom K, Cerrone M, Mironov S, Zugermayr M, Lopatin AN, Jalife J. Up-regulation of the inward rectifier K^+ current (I_{K1}) in the mouse heart accelerates and stabilizes rotors. *J Physiol*. 2007;578:315–326.
- Schulz R, Rassaf T, Massion PB, Kelm M, Balligand JL. Recent advances in the understanding of the role of nitric oxide in cardiovascular homeostasis. *Pharmacol Ther*. 2005;108:225–256.
- Gómez R, Núñez L, Vaquero M, Amorós I, Barana A, de Prada T, Macaya C, Maroto L, Rodríguez E, Caballero R, López-Farré A, Tamargo J, Delpón E. Nitric oxide inhibits Kv4.3 and human cardiac transient outward potassium current I_{to1} . *Cardiovasc Res*. 2008;80:375–384.
- Núñez L, Vaquero M, Gómez R, Caballero R, Mateos-Cáceres P, Macaya C, Iriepa I, Gálvez E, López-Farré A, Tamargo J, Delpón E. Nitric oxide blocks hKv1.5 channels by S-nitrosylation and by a cyclic GMP-dependent mechanism. *Cardiovasc Res*. 2006;72:80–89.
- Piao L, Li J, McLerie M, Lopatin AN. Cardiac I_{K1} underlies early action potential shortening during hypoxia in the mouse heart. *J Mol Cell Cardiol*. 2007;43:27–38.
- Hess DT, Matsumoto A, Kim SO, Marshall HE, Stamler JS. Protein S-nitrosylation: purview and parameters. *Nat Rev Mol Cell Biol*. 2005;6:150–166.
- Garneau L, Klein H, Parent L, Sauvé R. Contribution of cytosolic cysteine residues to the gating properties of the Kir2.1 inward rectifier. *Biophys J*. 2003;84:3717–3729.
- Lu T, Nguyen B, Zhang X, Yang J. Architecture of a K^+ channel inner pore revealed by stoichiometric covalent modification. *Neuron*. 1999;22:571–580.
- Kim YM, Guzik TJ, Zhang YH, Zhang MH, Kattach H, Ratnatunga C, Pillai R, Channon KM, Casadei B. A myocardial Nox2 containing NAD(P)H oxidase contributes to oxidative stress in human atrial fibrillation. *Circ Res*. 2005;97:629–636.
- Dobrev D, Graf E, Wettwer E, Himmel HM, Hála O, Doerfel C, Christ T, Schüler S, Ravens U. Molecular basis of downregulation of G-protein-coupled inward rectifying K^+ current $I_{K,ACh}$ in chronic human atrial fibrillation: decrease in GIRK4 mRNA correlates with reduced $I_{K,ACh}$ and muscarinic receptor-mediated shortening of action potentials. *Circulation*. 2001;104:2551–2557.
- Kuo A, Gulbis JM, Antcliff JF, Rahman T, Lowe ED, Zimmer J, Cuthbertson J, Ashcroft FM, Ezaki T, Doyle DA. Crystal structure of the potassium channel KirBac1.1 in the closed state. *Science*. 2003;300:1922–1926.
- Decher N, Renigunta V, Zuzarte M, Soom M, Heinemann SH, Timothy KW, Keating MT, Daut J, Sanguinetti MC, Splawski I. Impaired interaction between the slide helix and the C-terminus of Kir2.1: a novel mechanism of Andersen syndrome. *Cardiovasc Res*. 2007;75:748–757.
- Nekouzadeh A, Silva JR, Rudy Y. Modeling subunit cooperativity in opening of tetrameric ion channels. *Biophys J*. 2008;95:3510–3520.
- Malinski T. Understanding nitric oxide physiology in the heart: a nano-medical approach. *Am J Cardiol*. 2005;96:131–24i.